DOI: https://doi.org/10.33103/uot.ijccce.23.2.10

Whale Optimization Algorithm Enhances the Performance of Knee-Exoskeleton System Controlled by SMC

Zahraa Ali Waheed[1], Amjad Jaleel Humaidi [2]
[1,2]Control and Systems Engineering Department, University of Technology, Baghdad, Iraq
[1]cse.19.20@grad.uotechnology.edu.iq, [2]601116@uotechnology.edu.iq

***Abstract*—** *Physiotherapeutic exoskeleton devices have recently been developed to help people rehabilitate impaired limb mobility and replace the use of physiotherapists. Such systems are characterized by high nonlinear and time-varying coefficients. In order to cope with such difficult control challenges, a need arose for reliable nonlinear controllers. While in this study the Sliding Mode Control (SMC) was used to track the trajectory of the knee exoskeleton-system (KES) while having parameter uncertainty. In addition, the whale optimization algorithm (WOA) was introduced and developed to adjust the thickness design parameters for further optimization of its performance. The simulation was performed on a calculator using the MATLAB-Simulink program to conduct a comparative study between the optimal and Classical SMC where the results of comparison with the test parameters used by the SMC showed, the results of the proposed optimal SMC revealed that the positioning inaccuracy of the knee increased by 31.8807% and it follows from this result that the controller could successfully perform tracking the track well. Also, the control system created at the optimal thickness has a better dynamic performance than the classical thickness.*

Index Terms— *Optimal, Knee exoskeleton system, Whale optimization approach, Sliding mode control.*

I. INTRODUCTION

Joint dysfunction handicapped a large number of people every year due to a variety of factors. These individuals exhibit torque output and a disability to adjust mechanical opposition around the joints as signs of their muscle control ability. [1-4]. Therefore, many of these disabled patients can benefit from rehabilitation techniques to aid in their recovery from their conditions and return to their daily lives. [5]. The major causes of elbow impairments in people are accidents and diseases. Any of these scenarios has the unfortunate side effect of injuring the muscles or nerves. This ultimately results in problems with motor skills and paralysis. To address the issue of muscle and chord weakness, assistive , rehabilitative devices and gadgets were developed to aid in the mobility of handicappe people with varied disabilities. The programs are gradually included in the Neuro-rehabilitation process with the assistance of robotic devices. [6].

Exoskeletons, or wearable robots, can engage patients both physically and mentally [7]. These exoskeleton robotic systems work in conjunction with human parties [8]. Although research and development on exoskeleton system began in the 1960s, patients with motor impairments have only recently used them for functional surrogate and rehabilitation. [9-11] These exoskeletons are articulated mechanical devices that rely on sensors and actuators to function properly. Actuators capable of meeting the stroke and force prerequisite of a wearable exoskeletal or orthotic system are specifically developed to fit the size and weight of handicapped human body parts. Furthermore, the number of actuators required is determined by the number of joints that must be moved. [12].

Received 03/December/2022; Accepted 04/January/2023
 ISSN (Print) 1811-9212 ISSN (Online) 2617-3352

DOI: https://doi.org/10.33103/uot.ijccce.23.2.10

Furthermore, the computational and control design issues are predicated on the number of degrees of freedom (DoF) that human musculoskeletal systems have. As a result, the control system is critical for achieving an efficient design. To function successfully, the system must consider aspects such as how rapidly and where each limb travels, how well it can conform to its ambiance, and how much power each limb requires. These are all variables that have to considered [13].

As a result, developing a successful control model for exoskeleton systems necessitates the use of robust control. SMC control approach was applied in this work for the knee exoskeleton system. The Sliding mode control approach has been shown to be effective in the control of complicated and high order nonlinear systems in the face of uncertainty. The SMC control methods are used in a variety of applications [14-16].

The knee exoskeleton system-based systems have a high level of complexity and nonlinearity, as well as unpredictable parameters. Many scholars have approached various control solutions to handle the control difficulties of actuated uncertain mechanical systems. The following studies focus on the most modern control strategies knee exoskeleton system-actuated systems: Sherwani et al [2019] RISE on Exoskeleton Intelligently Communicating and Sensitive to Intention (EICoSI) designed and applied to rehabilitate impaired individuals at the knee joint. The recommended controller could achieve semi-global tracking subjected to unstructured disturbance [17]. Ajayi et al [2017] applied a bounded control strategy for the assistance and rehabilitation of patients due to partial and complete lower-limb motor function disorders. The assistant device is centered on the level of the knee and ankle joints. In order to estimate the joint angles, velocities, and torques [18]. Rifa etal [2012] designed a model reference adaptive controller (MRAC) to control lower-limb orthosis at the level of the knee level. The modeling of the shank-orthosis system has been developed considering the external torque as the human effort [19]. A. Chevalier et al [2014] presented motion-tracking control of the shank around the knee joint based on Fractional-Order Proportional-Integral (FOPI) controller. The objective of the controller is to regulate the shank angular position by applying desired torque to the knee joint [20]. S. Kaur et al. [2016] exposed the design of fractional-order-PID (FOPID) controller based on internal-mode-control (IMC) for motion control of the shank around the knee joint. Some design values of the FOPID controller have been determined using conventional IMC [21]. S. Mefoued et al. [2013] applied second-order-sliding -mode-control (SOSMC) to guarantee precise motion of knee joints to assist reduced-mobility persons due to weak functions of muscles. The parameters of the lower-limb orthosis model have been estimated using different techniques [22]. S. Mefoued [2014] presented Multi-Layer Perceptron Neural Network (MLPNN) to regulator the movements of the knee joint for flexion-extension. The proposed controller is an adaptive controller which can cope with the uncertainties of system parameters and it is a model-free controller which does not require the system's dynamic model [23]. S. Mefoued and D. Belkhiat [2019] have designed a robust controller based on sliding- mode-observer (SMO) to assist persons with weak mobility of knee joints. The study developed the dynamic-model of the lower-limb exoskeleton coupled with the leg of the patient [24]. H. Rifai et al [2016] exposed a control design based on the L1 adaptive controller for trajectory tracking of rehabilitation devices on the knee level. The desired trajectory is described by the therapeutic doctor. This study first conducted the design of a classical L1 adaptive controller [25]. S. M. Mahdi et al [2022] used the concept of synergetic theory to design an adaptive synergetic controller for motion control exoskeleton device to rehabilitate people who suffer weak mobility in the knee joint [26]. A. S. Aljuboury et al. [2022] proposed an observer-based model reference adaptive control (MRAC) for motion control of the exoskeleton knee-assistive device for rehabilitation of weak mobility in the lower-limb part [27]. N. A. Alawad et al [2022] applied a modified version of active disturbance rejection control (ADRC) to control the movement of the shank around the knee joint using an exoskeleton system [28].

Received 03/December/2022; Accepted 04/January/2023

ISSN (Print) 1811-9212 ISSN (Online) 2617-3352

DOI: https://doi.org/10.33103/uot.ijccce.23.2.10

SMC has been evolved and optimized in this paper based on the whale optimization algorithm for movement control of the knee joint using a wearable exoskeleton rehabilitation system. The following points highlight the main contributions of this study:

(I) Evolution of SMC-based control laws to evidence error trajectories of the initial conditions to zero balance points in the specified time.

(II) Evolution an optimization algorithm based on WOA to tune the design parameters of the knee exoskeleton-system to improve the dynamic performance of the controlled-system.

The article is structured as follows: Part II introduces and analyzes a mathematical model of knee motion. The control design and analysis methodology are presented in III. The IV part established the WOA-based optimization algorithm. Numerical simulations are shown in the V part, and the last part of this study is concluded.

II. MATHEMATICAL MODEL

The system is comprised of the human-shank and the stereophonic actuated orthosis, as depicted in *Fig. 1*. The orthosis is a mechanical device that is fastened to the wearer's leg with braces and fits the wearer's leg perfectly. It is powered by an actuator, and the entire system moves in unison. For the goal of rehabilitation, the system is designed to carry out flexion extension movements of the human-shank [6].

The upper portion functions like the thigh, constant over the x-axis and powered by an actuator, enabling the knee joint to flex/extend. The lower end, with its angle (θ) of mobility-limited between 0° and 120°, serves as a shank-foot attached to the exoskeleton. The two reference coordinate systems knee joint moves in the global frame ($\vec{x}^f, \vec{y}^f, \vec{z}^f$) which is a fixed coordinate system centered on the earth, and the exoskeleton frame ($\vec{x}^s, \vec{y}^s, \vec{z}^s$) such that the orientations of $\vec{y}^f$ and $\vec{y}^s$ coincide:

The angle of total extension is represented by 0°; the angle of rest is represented by 90°; and the angle of maximum flexion of the knee is represented by 120° [28].

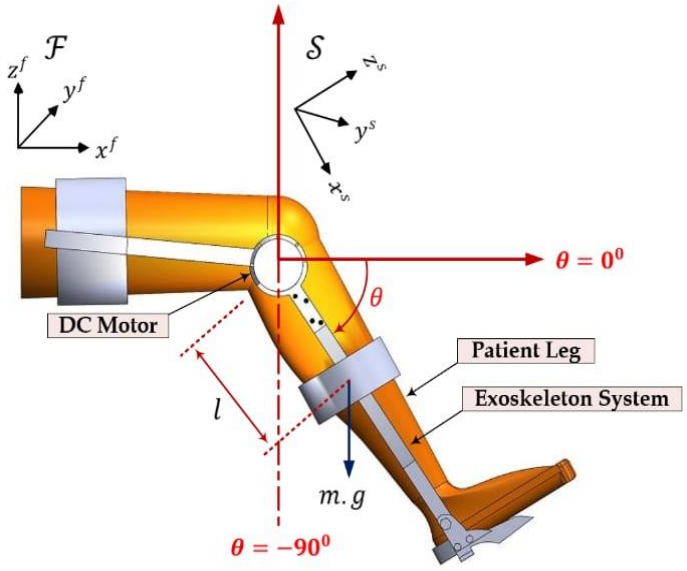

FIG. 1. A PERSON IN A SITTING POSITION WEARING THE EXOSKELETON SYSTEM [26].

Fig. 1 was used to generate the dynamic model of the exoskeleton and the human leg. The Euler- Lagrange equation gives the "generalized" equations of motion as [24, 26]:

Received 03/December/2022; Accepted 04/January/2023

ISSN (Print) 1811-9212 ISSN (Online) 2617-3352

DOI: https://doi.org/10.33103/uot.ijccce.23.2.10

$$\frac{d}{dt}\frac{\partial L}{\partial \dot{q}} - \frac{\partial L}{\partial q} = \tau_{ext} \quad (1)$$

where τ_{ext} is the external torque applied to the system and L_i is the general Lagrange equation which can be defined as [17]:

$$L_i = E_{ki} - E_{gi} \quad (2)$$

where E_{ki} and E_{gi} indicate the kinetic and gravitational energies of the leg and exoskeleton respectively [17].

$$E_{ki} = \frac{1}{2} J_i \dot{\theta}^2 \quad (3)$$

$$E_{gi} = g\, m_i l_i (1 - sin\,\theta) \quad (4)$$

Substitute eq. (3), (4) into eq. (2) donate eq. (5)

$$L_i = \frac{1}{2} J\dot{\theta}^2 - g\, m_i l_i (1 - sin\,\theta) \quad (5)$$

where J_i is the inertia of the human leg and exoskeleton, θ_k is the angle of mobility, m_{ik} , g_k and l_{ik} symbolize the mass of the human leg and exoskeleton, the acceleration due to gravity, and the distance amongst the knee joint and the center-of-gravity, respectively.

$$\frac{\partial L}{\partial \dot{\theta}} = J_i\, \dot{\theta} \quad (6)$$

$$\frac{d}{dt}\frac{\partial L}{\partial \dot{\theta}} = J_i \ddot{\theta} \quad (7)$$

$$\frac{\partial L}{\partial \theta} = g\, m_i l_i\, cos\,\theta \quad (8)$$

Substituting Eq. (7) and Eq. (8) into Eq. (1) to have

$$J_i \ddot{\theta} - g\, m_i l_i\, cos\,\theta = \tau_{ext} \quad (9)$$

$$\tau_{ext} = \tau_{fi} + \tau_i \quad (10)$$

By using Eq. (10),Eq.(9)becomes

$$J_i \ddot{\theta} - g\, m_i l_i\, cos\,\theta = \tau_{fi} + \tau_i \quad (11)$$

where τ_{fi} and τ_i symbolize the friction control torque and motor control torque, Consecutively [17].

$$\tau_{fi} = -f_S \,\text{sign}\,\dot{\theta} - f_v \dot{\theta} \quad (12)$$

$$\tau_i = \tau_k \quad (13)$$

$$\tau_g = g\, m_i l_i \quad (14)$$

where τ_g is the system's gravitational torque, f_s and f_v represent the solid and viscous friction coefficients and the (sign) function is the traditional signum function.

Substitution Eq. (12), Eq.(13) and Eq.(14) into Eq.(11) gives

$$J\ddot{\theta} - \tau_g \cos\theta = -f_S \,\text{sign}\,\dot{\theta} - f_v \dot{\theta} + \tau_k \quad (15)$$

The human leg and exoskeleton dynamics are included in the system model.

$$J\ddot{\theta} + f_S \,\text{sign}\,\dot{\theta} + f_v \dot{\theta} - \tau_g \,\text{Cos}\,\theta = \tau_k \quad (16)$$

In the robotic form as follows Equation (16) can be written:

$$M(\theta)\ddot{\theta} + f\left(\theta, \dot{\theta}\right) + G(\theta) = B(u) \quad (17)$$

where $M(\theta) = J$ is inertia matrix, $f(\theta, \dot{\theta}) = -f_S\, sign\dot{\theta} - B_i$ represents the friction force,$G(\theta) = \tau_g \cos\theta$ is the gravity force at the knee joint, $B(u) = \tau_k$ represents the torque acting at the knee joint. Based on Eq. (17), one can express the equation in terms of acceleration of angular positions as follows:

Received 03/December/2022; Accepted 04/January/2023

ISSN (Print) 1811-9212 ISSN (Online) 2617-3352

DOI: https://doi.org/10.33103/uot.ijccce.23.2.10

$$\ddot{\theta} = M(\theta)^{-1}\left(\tau_k - f\left(\theta,\dot{\theta}\right) - G(\theta)\right) \quad (18)$$

In state variables representation, Eq.(17)can be formulated as follows:

$$\dot{x}_1 = \dot{\theta} = x_2 \quad (19)$$

$$\dot{x}_2 = \ddot{\theta} = \frac{1}{J}\left[\tau_k - f_s sign(x_2) - f_v(x_2) + \tau_g \cos(x_1)\right] \quad (20)$$

where x_1 denotes the angular posture of the knee joint (θ), and the state variable x_2 represents the angular velocity of the knee joint.

III. CONTROLLER DESIGN

In this section presented the SMC design for the knee-exoskeleton system:

Let e be the variation between the current location $x_1 = \theta$ and the reference path $x_{1d} = \theta_d$ as shown

$$e = x_1 - x_{1d} \quad (21)$$

The derivative of the error equation gives

$$\dot{e} = \dot{x}_1 - \dot{x}_{1d} = x_2 - \dot{x}_{1d} \quad (22)$$

$$\ddot{e} = \dot{x}_2 - \ddot{x}_{1d} \quad (23)$$

For this system, the sliding surface is assumed to be

$$s = c\, e + \dot{e} \quad (24)$$

Apply the first-time derivative of Eq. (24)

$$\dot{s} = c\, \dot{e} + \ddot{e} \quad (25)$$

$$\Rightarrow \dot{s} = c\, \dot{e} + \dot{x}_2 - \ddot{x}_{1d} \quad (26)$$

While c is a scalar design value. Using Eq.(20), Eq.(26) turn out

$$\Rightarrow \dot{s} = c\, \dot{e} + \frac{1}{J}\left(\tau_k - f_v\, x_2 - f_s\, sign(x_2) + \tau_g \cos(x_1)\right) - \ddot{x}_{1d} \quad (27)$$

Let$\tau_k = u$, Eq.(27) becomes

$$\dot{s} = c\, \dot{e} + \frac{1}{J}\left(u - f_v\, x_2 - f_s\, sign(x_2) + \tau_g \cos(x_1)\right) - \ddot{x}_{1d} \quad (28)$$

In the SMC (Sliding Mode Control) technique, the control law (u) is defined by

$$u = u_{eq} + u_{sw} \quad (29)$$

where, $u_{eq}$and u_{sw} are the equivalent and switching control parts,

Now choose the two elements of control action:

$$u_{eq} = J\left(f_v\, x_2/J + f_s\, sign(x_2)/J - \tau_g \cos(x_1)/J - c\, \dot{e} + \ddot{x}_{1d}\right) \quad (30)$$

$$u_{sw} = -\beta_1\, sgn\,(s) \quad (31)$$

$$u = J\left(f_v\, x_2/J + f_s\, sign(x_2)/J - \tau_g \cos(x_1)/J - c\, \dot{e} + \ddot{x}_{1d}\right) - \beta_1 sign\,(s) \quad (32)$$

SMC is a discontinuous control approach that uses variable structure synthesis to develop it. The presence of a sliding surface represents a turning point in SMC design. When the erroneous state's trajectory is driven to approach this sliding surface, it asymptotically slides to a point of equilibrium. The SMC has highly resilient features against uncertainty in its system parameters and, thanks to its bounded matched trait, it also resists external disruption [29].

IV. WHALE OPTIMIZATION APPROACH

The notion of whale social behaviour serves as the foundation for the recently created whale optimization approach (WOA), a novel search method. Of all whale species, humpback whales are the

Received 03/December/2022; Accepted 04/January/2023
 ISSN (Print) 1811-9212 ISSN (Online) 2617-3352

DOI: https://doi.org/10.33103/uot.ijccce.23.2.10

biggest. Whales take pleasure in pursuing tiny fish. The method of humpback whale hunting is bubble net nutrition. The twisting bubble net nutrition method is mathematically presented by WOA. Humpback whales demonstrate some crucial behaviour while they are hunting. *Fig. 2* illustrates how to forage by forming distinctive bubbles along a path that is circular or shaped like a "9." The following is the mathematical model optimization algorithm for the proposed WOA estimate: [30-32].

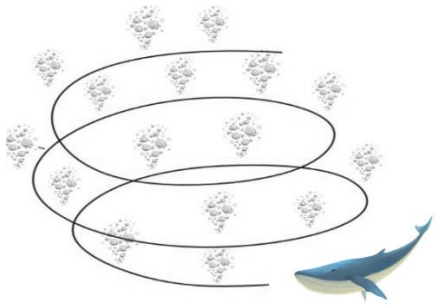

FIG. 2. BUBBLE-NET FEEDING BEHAVIOR OF HUMPBACK WHALES.

A. Encircling Prey

While hunting, humpback whales encircle their prey, and the WOA algorithm assumes that the best candidate solution is close to the target prey or target prey because the optimal design position in the search space is previously unknown. The mathematical representation of the encircling behaviour model used to update the attitude of other whales toward the best search agent is as follows:

$$\vec{D} = \left|\vec{C}\,.\vec{X}\,(t) - \vec{X}\,(t)\right| \quad (33)$$

$$\vec{X}(t+1) = \overrightarrow{X^*}(t) - \vec{A}.\vec{D} \quad (34)$$

$$\vec{A} = 2\vec{a}\,\vec{r} - \vec{a} \quad (35)$$

$$\vec{C} = 2\,\vec{r} \quad (36)$$

where $\overrightarrow{X^*}$ the public location vector, $\vec{X}$ denote whale locate, t allocates the present iteration, $\vec{a}$ illustrate linearly diminutive within the range of 2 to 0 during iteration, and r is a random number evenly distributed in the domain of [0, 1] [33].

B. Exploitation Phase

The behavior of the humpback whales' bubble network is demonstrated in the following parts.

- **Shrinking encircling mechanism:**

This demeanor is attained by diminishing the amount of $\overrightarrow{A}$. Notice that the variation range of $\overrightarrow{A}$ is also reduced by $\overrightarrow{a}$. Setting random values for $\overrightarrow{A}$ in [-1, 1], the next location of a search agent can be specified anywhere between the pristine location of the agent and the location of the best present agent.

- **Spiral updating location:**

This method first computes the distance between the whale at (X, Y) and the prey at (X*, Y*). To imitative the spiral movement of humpback whales, a spiral equation is created between the position of the whale and prey, as shown below:

$$\vec{X}\,(t+1) = \overrightarrow{D'}\,e^{bl}\cos(2\pi l) + \overrightarrow{X^*}\,(t) \quad (37)$$

where $\vec{D} = \left|\vec{X}^*\,(t) - \vec{X}\,(t)\right|$ denotes the i-th whales' proximity to the prey (perfect solution), b is an enduring that defines the format of the hyperbolic spiral, and t is a random number in [-1,1][34].

It's important to note that humpback whale travel in a spiral-shaped pattern and swim in a smaller circle around their prey. Assume there is a 50% chance of selecting either the spiral model or

Received 03/December/2022; Accepted 04/January/2023

ISSN (Print) 1811-9212 ISSN (Online) 2617-3352

DOI: https://doi.org/10.33103/uot.ijccce.23.2.10

a shrinking encircling mechanism to update the location of whales over optimization to simulate this concurrent activity. The mathematical representation is as follows:

$$\vec{X}(t+1) = \begin{cases} \overrightarrow{X^*}(t) - \vec{A}.\vec{D} & p < 0.5 \\ \overrightarrow{D'}\, e^{bl}\, cos(2\pi l) + \overrightarrow{X^*}(t) & p \geq 0.5 \end{cases} \quad (38)$$

where p is a random number in [0,1].

C. Exploration Phase

The related algorithm based on the variance of the ($\vec{A}$) a vector may be used to locate prey. Humpback whales search unspecified depending on their proximity to one another. The ($\vec{A}$) with random values bigger than 1 or below -1 will cause the search factor to wander far from a reference whale. In disparity with the exploitation phase, whales change the position of a search factor during the exploration phase based on a randomly selected search agent as opposed to the ideal search factor. The WOA algorithm may carry out a global search thanks to this technique and | ($\vec{A}$) |>1. Here is the mathematical model:

$$\vec{D} = \left|\vec{C}\,.\vec{X}(t) - \vec{X}(t)\right| \quad (39)$$

$$\vec{X}(t+1) = \vec{X}rand - \vec{A}.\vec{D} \quad (40)$$

The WOA algorithm's pseudo-code is shown below:

Algorithm 2: WOA

Input data, Number of Maxiter and Population, etc.
Initialize the whales population Xi (i = 1, 2,..., n)
Initialize a, A, C, l and p
Calculate the fitness of each search agent
X= the best search agent*
while (it < Maxiter)
for each search agent
if (p < 0.5)
if (|A| < 1)
*Update the position of the current search agent by the equation (*37*)*
else if (|A| ≥ 1)
Select a random search agent (X_rand)
*Update the position of the current search agent by the equation (*36*)*
end
else if (p ≥ 0.5)
*Update the position of the current search agent by the equation (*40 *)*
End

The numerical values for the WOA algorithm parameter are listed in Table I.

TABLE I. TEST MODEL SPECIFICATIONS AND TEST CONDITIONS

WOA Parameter	Amount
Random esteems	r_1 , r_2
Pop size	30
Ite No.	300

V. SIMULATIONS

The following parameters of the Exo Skeleton model simulation were employed, along with the suggested controller and exoskeleton responses, in Matlab/Simulink. The knee-Exoskeleton system's

Received 03/December/2022; Accepted 04/January/2023
 ISSN (Print) 1811-9212 ISSN (Online) 2617-3352

DOI: https://doi.org/10.33103/uot.ijccce.23.2.10

open-loop test is depicted in *Fig. 3*. A unit-step input method is used to control the system. The output response, indicated by angular displacement x1, is shown in *Fig. 3* to have started at zero. However, the response settles swiftly immediately after three seconds to reach over 1.6 rad. The numerical values for the knee-Exoskeleton system example are listed in Table II.

TABLE II. NUMERICAL VALUES OF SYSTEM PARAMETERS [24]

Coefficient	Value	Unit
J	0.348	Kgm^2
f_v	0.872	Nms/rad
f_s	0.998	Nms/rad
τ_g	3.445	Nm

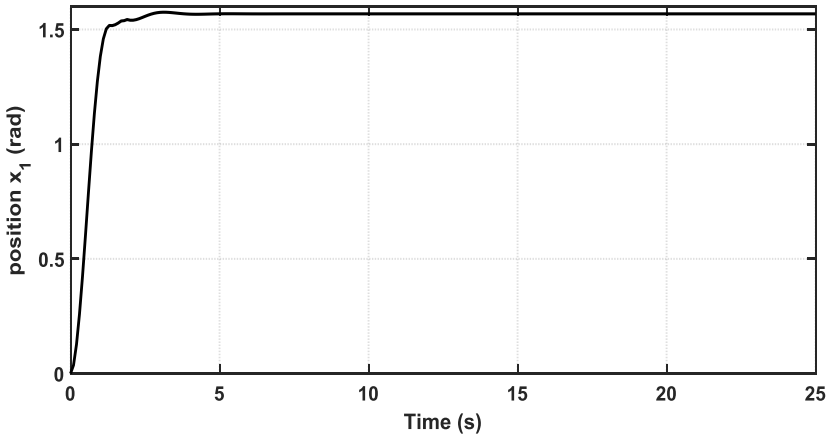

FIG. 3. OPEN LOOP RESPONSE.

Finding the ideal design parameter values to get the lowest RMSE is the aim of an optimization strategy. *Fig. 4* depicts how the index function for SMC behaves.

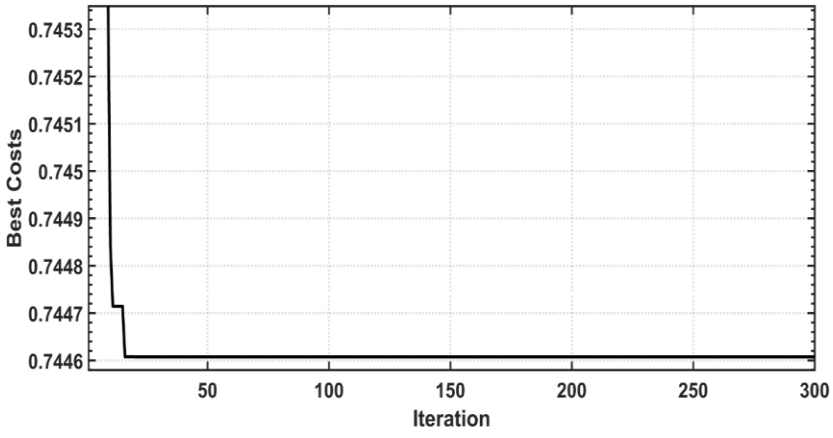

FIG. 4. COST FUNCTION FOR A CONTROLLED SYSTEM PREMISED ON SMC.

The knee-exoskeleton-system design parameters, as defined by SMC, are shown in Table III. The first collection of design factors was discovered using the WOA algorithm, while the second set was discovered using the trial-and-error technique. The ideal design parameter values of the WOA approaches are translated to the appropriate design factors of the controllers to provide the system with the best possible control. It projects a trajectory using a sine wave as an input.

Received 03/December/2022; Accepted 04/January/2023

ISSN (Print) 1811-9212 ISSN (Online) 2617-3352

DOI: https://doi.org/10.33103/uot.ijccce.23.2.10

TABLE III. SETTING OF DESIGN PARAMETERS FOR DIFFERENT CONTROLLERS OF KNEE-EXOSKELETON SYSTEM

SMC Controller Coefficient	Optimal Values Value	SMC Controller Coefficient	Experimental Values
C	16.5382	C	10
β_1	561.14	β_1	100

Fig. 5 depicts the behaviour of angular positions based on optimal and non-optimal SMC. It makes clear that the dynamic echo obtained by optimal SMC improves that based on the experimental procedure. The chattering phenomenon can be observed in the response of angular displacement in *Fig. 5*. *Fig. 6* demonstrates the tracking error of the knee exoskeleton system as it is regulated using optimal and classical SMC (e). *Fig. 6* clearly shows that the RMSE (0.0297) in the optimal case is less than the RMSE (0.0436) in the classical case.

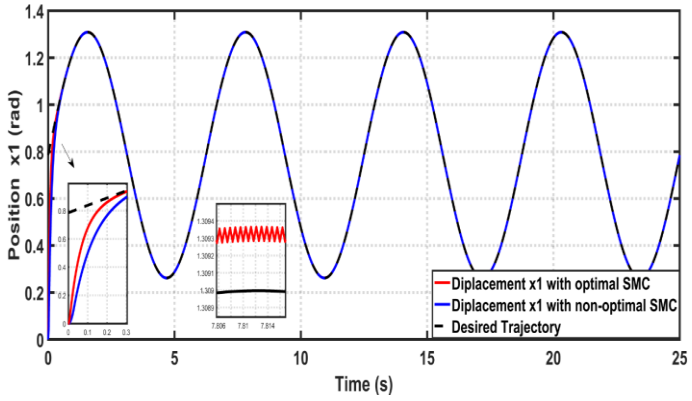

FIG. 5. BEHAVIORS OF ANGULAR POSITION OF CONTROLLED SYSTEM BASED ON SMC FOR BOTH OPTIMAL AND NON-OPTIMAL PROCEDURES.

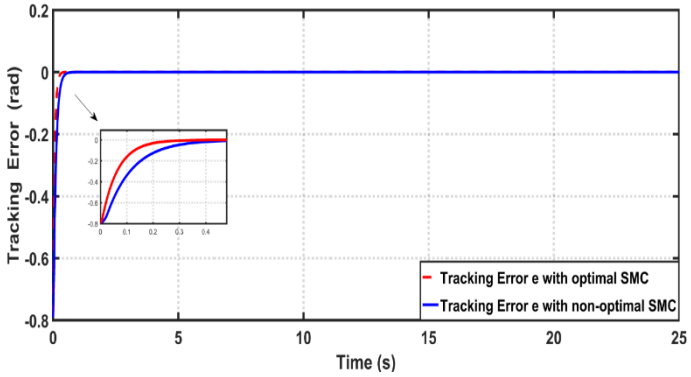

FIG. 6. SMC TRACKING ERROR.

Fig. 7 explains the corresponding control action effect. Chattering phenomena is obvious in *Fig. 7* which means the sliding variable trajectory crosses the zero and slides on it. In *Fig. 8*, the sliding variable trajectory in the phase plane is show, where the sliding phase comes after the reaching phase and the effects of chattering on the system state while it tracks the desired input.

Received 03/December/2022; Accepted 04/January/2023

ISSN (Print) 1811-9212 ISSN (Online) 2617-3352

DOI: https://doi.org/10.33103/uot.ijccce.23.2.10

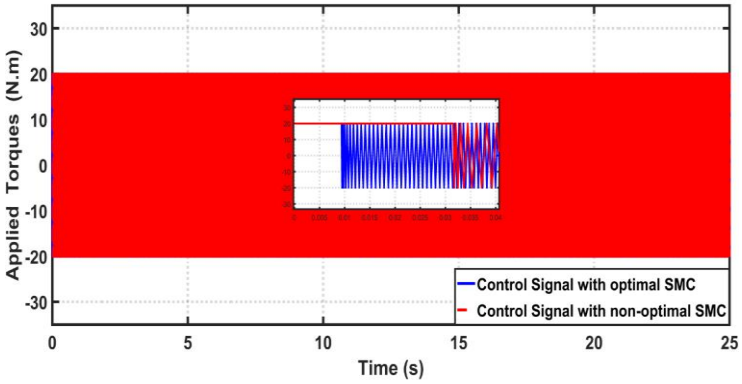

FIG. 7. BEHAVIOR OF CONTROL SIGNALS FOR CONTROLLED KNEE-EXOSKELETON SYSTEM BASED ON SMC FOR BOTH OPTIMAL AND NON-OPTIMAL SETTINGS.

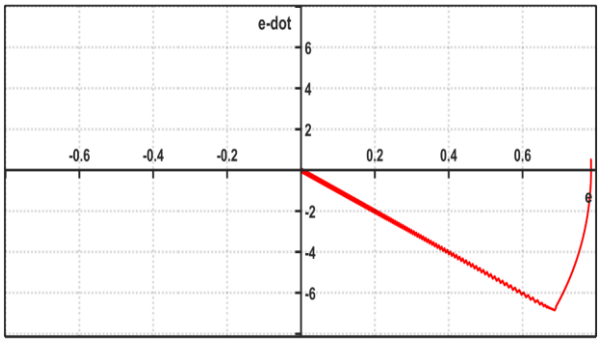

FIG. 8. KNEE SLIDING SURFACE FOR NON-OPTIMAL.

VI. CONCLUSIONS

In this research, a control scheme is designed to track the control of the knee-assisted rehabilitation pathway system. The control laws are developed according to the dynamical Lagrangian-based stability analysis. The famous strong sliding position control device is adopted to control the outer structure position control. Where the design parameters of the proposed controllers were set based on two types, the classic setup is the first type of setup that depends on the case and error method, while the other setup is based on WOA, where the comparison results showed between the two types that the WOA (optimal) tuner can significantly improve the performance of the proposed controllers with a classical ratio that increased by 31.8807%. From this result that the controller can successfully perform tracking well. Also, the control system created with the optimal thickness has better dynamic performance than the classic thickness. The next step of this work will be to apply this controller to the real system and enhance the performance of the controlled system by using adaptive sliding mode control.

REFERENCES

[1] A. M. Mohammad and S. A. AL-Samarraie, "Robust controller design for flexible joint based on back-stepping approach," *Iraqi J. Comput. Commun. Control Syst. Eng.*, vol. 20, no. 2, pp. 58–73, 2020.

[2] R. Nasiri, M. Shushtari, and A. Arami, "An adaptive assistance controller to optimize the exoskeleton contribution in rehabilitation," *Robotics*, vol. 10, no. 3, p. 95, 2021.

[3] S. S. Hassan, K. K. Resan, and A. Z. Mahdi, "Design and Analysis of Knee Ankle Foot Orthosis (KAFO) for Paraplegia Person," *Eng. Tech. J.*, vol. 31, no. 8, 2013.

[4] M. Q. Kadhim and M. Y. Hassan, "Design and optimization of backstepping controller applied to autonomous quadrotor," in *IOP Conference Series: Materials Science and Engineering*, vol. 881, no. 1, p. 12128, 2020.

[5] H. I. Ali, A. F. Hasan, and H. M. Jassim, "Optimal H2PID controller design for human swing leg system using cultural algorithm," *J. Eng. Sci. Technol.*, vol. 15, no. 4, pp. 2270–2288, 2020.

[6] C. T. Moritz and F. Ambrosio, "Regenerative Rehabilitation: Combining Stem Cell Therapies and Activity Dependent Stimulation," *Pediatr. Phys. Ther. Off. Publ. Sect. Pediatr. Am. Phys. Ther. Assoc.*, vol. 29, no. Suppl 3 IV STEP 2016 CONFERENCE PROCEEDINGS, p. S10, 2017.

Received 03/December/2022; Accepted 04/January/2023

ISSN (Print) 1811-9212 ISSN (Online) 2617-3352

DOI: https://doi.org/10.33103/uot.ijccce.23.2.10

[7] J. L. Collinger, S. Foldes, T. M. Bruns, B. Wodlinger, R. Gaunt, and D. J. Weber, "Neuroprosthetic technology for individuals with spinal cord injury," *J. Spinal Cord Med.*, vol. 36, no. 4, pp. 258–272, 2013.
[8] M. A. Salman and S. K. Kadhim, "Optimal Backstepping Controller Design for Prosthetic Knee Joint," *J. Eur. des Systèmes Autom.*, vol. 55, no. 1, pp. 49–59, 2022.
[9] M. Y. Hassan and Z. A. Karam, "Modeling and force-position controller design of rehabilitation robot for human arm movements," *Eng. Technol. J.*, vol. 32, no. 8 Part (A) Engineering, 2014.
[10] M. L. Jones *et al.*, "Activity-based therapy for recovery of walking in individuals with chronic spinal cord injury: results from a randomized clinical trial," *Arch. Phys. Med. Rehabil.*, vol. 95, no. 12, pp. 2239–2246, 2014.
[11] N. A. Alawad, A. J. Humaidi, A. S. M. Al-Obaidi, and A. S. Alaraji, "Active Disturbance Rejection Control of Wearable Lower-Limb System Based on Reduced ESO," *Indones. J. Sci. Technol.*, vol. 7, no. 2, pp. 203–218, 2022, doi: 10.17509/ijost.v7i2.46435.
[12] H. Herr, "Exoskeletons and orthoses: Classification, design challenges and future directions," *J. Neuroeng. Rehabil.*, vol. 6, no. 1, pp. 1–9, 2009, doi: 10.1186/1743-0003-6-21.
[13] K. Kim, P. Spieler, E.-S. Lupu, A. Ramezani, and S.-J. Chung, "A bipedal walking robot that can fly, slackline, and skateboard," *Sci. Robot.*, vol. 6, no. 59, p. eabf8136, 2021.
[14] D. H. Tohma and A. K. Hamoudi, "Design of Adaptive Sliding Mode Controller for Uncertain Pendulum System," *Eng. Technol. J.*, vol. 39, no. 3A, pp. 355–369, 2021, doi: 10.30684/etj.v39i3a.1546.
[15] A. J. Humaidi, E. N. Tala'at, A. Q. Al-Dujaili, D. A. Pereira, and I. K. Ibraheem, "Design of backstepping control based on adaptive observer for underactuated system," in *2020 7th International Conference on Control, Decision and Information Technologies (CoDIT)*, 2020, vol. 1, pp. 288–293.
[16] K. Adamiak, "Chattering-Free Reference Sliding Variable-Based SMC," *Math. Probl. Eng.*, vol. 2020, p. 3454090, 2020, doi: 10.1155/2020/3454090.
[17] K. I. K. Sherwani, N. Kumar, A. Chemori, M. Khan, and S. Mohammed, "RISE-based adaptive control for EICoSI exoskeleton to assist knee joint mobility," *Rob. Auton. Syst.*, vol. 124, 2020, doi: 10.1016/j.robot.2019.103354.
[18] M. O. Ajayi, K. Djouani, and Y. Hamam, "Bounded Control of an Actuated Lower-Limb Exoskeleton," *J. Robot.*, vol. 2017, p. 2423643, 2017, doi: 10.1155/2017/2423643.
[19] H. Rifaï, S. Mohammed, B. Daachi, and Y. Amirat, "Adaptive control of a human-driven knee joint orthosis," *Proc. - IEEE Int. Conf. Robot. Autom.*, pp. 2486–2491, 2012, doi: 10.1109/ICRA.2012.6225064.
[20] A. Chevalier, C. M. Ionescu, and R. De Keyser, "Analysis of robustness to gain variation in a fractional-order PI controller for knee joint motion," *2014 Int. Conf. Fract. Differ. Its Appl. ICFDA 2014*, 2014, doi: 10.1109/ICFDA.2014.6967359.
[21] S. Kaur, S. Sagar, and S. Sondhi, "Internal model control based fractional order PID controller for knee joint motion," *11th Int. Conf. Ind. Inf. Syst. ICIIS 2016 - Conf. Proc.*, vol. 2018-Janua, pp. 318–322, 2016, doi: 10.1109/ICIINFS.2016.8262958.
[22] S. Mefoued, S. Mohammed, and Y. Amirat, "Toward movement restoration of knee joint using robust control of powered orthosis," *IEEE Trans. Control Syst. Technol.*, vol. 21, no. 6, pp. 2156–2168, 2013, doi: 10.1109/TCST.2012.2228194.
[23] S. Mefoued, "A robust adaptive neural control scheme to drive an actuated orthosis for assistance of knee movements," *Neurocomputing*, vol. 140, pp. 27–40, 2014, doi: https://doi.org/10.1016/j.neucom.2014.03.038.
[24] S. Mefoued and D. E. C. Belkhiat, "A Robust Control Scheme Based on Sliding Mode Observer to Drive a Knee-Exoskeleton," *Asian J. Control*, vol. 21, no. 1, pp. 439–455, 2019, doi: 10.1002/asjc.1950.
[25] H. Rifai, M. S. Ben Abdessalem, A. Chemori, S. Mohammed, and Y. Amirat, "Augmented -1 adaptive control of an actuated knee joint exoskeleton: From design to real-time experiments," *Proc. - IEEE Int. Conf. Robot. Autom.*, vol. 2016-June, pp. 5708–5714, 2016, doi: 10.1109/ICRA.2016.7487794.
[26] S. M. Mahdi, N. Q. Yousif, A. A. Oglah, M. E. Sadiq, A. J. Humaidi, and A. T. Azar, "Adaptive Synergetic Motion Control for Wearable Knee- Assistive System: A Rehabilitation of Disabled Patients," *Actuators*, vol. 11, no. 7, 2022, doi: 10.3390/act11070176.
[27] A. S. Aljuboury, A. H. Hameed, A. R. Ajel, A. J. Humaidi, A. Alkhayyat, and A. K. A. Mhdawi, "Robust Adaptive Control of Knee Exoskeleton-Assistant System Based on Nonlinear Disturbance Observer," *Actuators*, vol. 11, no. 3, 2022, doi: 10.3390/act11030078.
[28] N. A. Alawad, A. J. Humaidi, and A. S. Alaraji, "Observer Sliding Mode Control Design for lower Exoskeleton system: Rehabilitation Case," *J. Robot. Control*, vol. 3, no. 4, pp. 476–482, 2022.
[29] A. A. Al-Qassar *et al.*, "Finite-time control of wing-rock motion for delta wing aircraft based on whale-optimization algorithm," *Indones. J. Sci. Technol.*, vol. 6, no. 3, pp. 441–456, 2021, doi: 10.17509/ijost.v6i3.37922.
[30] S. Mirjalili and A. Lewis, "The Whale Optimization Algorithm," *Adv. Eng. Softw.*, vol. 95, pp. 51–67, 2016, doi: 10.1016/j.advengsoft.2016.01.008.
[31] N. Rana, M. S. A. Latiff, S. M. Abdulhamid, and H. Chiroma, *Whale optimization algorithm: a systematic review of contemporary applications, modifications and developments*, vol. 32, no. 20. Springer London, 2020. doi: 10.1007/s00521-020-04849-z.
[32] R. K. Khadanga, A. Kumar, and S. Panda, "A novel modified whale optimization algorithm for load frequency controller design of a two-area power system composing of PV grid and thermal generator," *Neural Comput. Appl.*, vol. 32, no. 12, pp. 8205–8216, 2020, doi: 10.1007/s00521-019-04321-7.
[33] A. M. Mosaad, M. A. Attia, and A. Y. Abdelaziz, "Whale optimization algorithm to tune PID and PIDA controllers on AVR system," Ain Shams Eng. J., vol. 10, no. 4, pp. 755–767, 2019, doi: 10.1016/j.asej.2019.07.004.

Received 03/December/2022; Accepted 04/January/2023
 ISSN (Print) 1811-9212 *ISSN (Online) 2617-3352*